

Mesenchymal stem cells inhibited the apoptosis of alveolar epithelial cells caused by ARDS through CXCL12/CXCR4 axis

Xiqiang He, Chenyan Li, Hua Yin, Xiaojun Tan, Jun Yi, Shujun Tian, Yan Wang, and Jian Liu

Surgical intensive care unit, Xiangtan Central Hospital, China

ABSTRACT

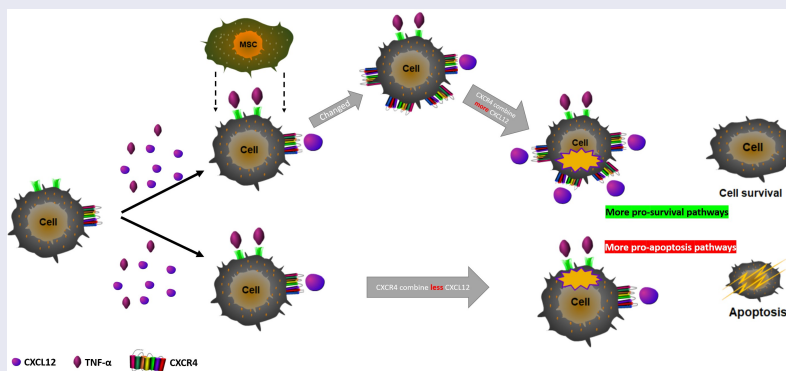
Mesenchymal stem cells (MSCs) have a wide range of anti-inflammatory and immunomodulatory effects and have been observed to have potential therapeutic potential in the clinical treatment of various diseases. We pretreated lung cancer cells A549 with tumor necrosis factor (TNF- α), knocked down the key chemokine receptor CXCR4 on MSCs using lentivirus, and induced acute respiratory distress syndrome (ARDS) mouse model using lipopolysaccharide (LPS) and CXCL12 expression in vivo by adeno-associated virus (AAV-rh10) infection in mice. By co-culturing the MSCs with A549 and in vivo experiments, we observed the effects of MSCs on cell biological functions after inflammatory stimulation, oxidative stress, and the amelioration of lung injury in ARDS mice. TNF- α inhibited A549 proliferation and promoted apoptosis, scorch death-related factor activity, and oxidative stress factor were increased and CXCL12 levels in the cell supernatant were decreased. The co-culture of MSCs was able to increase cell activity and decrease oxidative stress factor levels, and this effect was not present after the knockdown of CXCR4 in MSCs. In vivo transplantation of MSCs significantly attenuated lung injury in ARDS, inhibited serum pro-inflammatory factors in mice, and down-regulated expression of apoptotic and focal factors in lung tissues while blocking CXCR4 or CXCL12 lost the repairing effect of MSCs on ARDS lung tissues. After the co-culture of MSC and lung cancer cells, the expression of CXCR4 on the surface of lung cancer cells was significantly increased, and more CXCR4 and CXCL12 acted together to activate more pro-survival pathways and inhibit apoptosis induced by TNF- α .

ARTICLE HISTORY

Received 11 January 2022
Revised 8 March 2022
Accepted 9 March 2022

KEYWORDS

Mesenchymal stem cells;
CXCL12/CXCR4 signal axis;
acute respiratory distress
syndrome; apoptosis




Introduction

Acute respiratory distress syndrome (ARDS), which is an inflammatory injury of the lungs, is characterized by acute respiratory failure that can cause a sudden decrease in lung compliance and CO₂ and reduced lung tissue inflation, leading to hypoxemia, non-cardiogenic pulmonary edema, and acute onset of mechanical ventilation [1]. ARDS is caused by bacterial or viral infection,

chemical destruction of the lungs, extrapulmonary damage, or inflammation. The pathogenesis of ARDS is currently unclear [2].

There is no specific drug to reduce the mortality of ARDS. Moreover, currently used drugs often have serious side effects, such as acute kidney injury [3]. However, several prospective therapeutic methods are imminently being explored, such as anticoagulation, immunomodulatory methods

CONTACT Jian Liu  jianliuli00@163.com  Surgical intensive care unit, Xiangtan Central Hospital, 120 Heping Road, Yuhu District, Xiangtan 411100, China
 Supplemental data for this article can be accessed [here](#)

© 2022 The Author(s). Published by Informa UK Limited, trading as Taylor & Francis Group.
This is an Open Access article distributed under the terms of the Creative Commons Attribution-NonCommercial License (<http://creativecommons.org/licenses/by-nc/4.0/>), which permits unrestricted non-commercial use, distribution, and reproduction in any medium, provided the original work is properly cited.

(e.g., IL-6 receptor blockers), reusable drugs (e.g., azithromycin), convalescent plasma, and monoclonal antibodies. An increasing number of studies have identified potential promising treatments for ARDS in clinical practice [4]. A study of 167 patients with ARDS compared high-dose vitamin C with placebo; compared with placebo, patients in the vitamin C treatment group had a notable reduction in 28-day mortality (30% vs. 46%, $p = 0.03$) [5].

Mesenchymal stem cells are non-hematopoietic stem cells isolated from bone marrow and other tissues and have immunomodulatory and regenerative properties that could directly inhibit disease damage to organs or indirectly inhibit the release of harmful factors by reducing cell death, to effectively avoid the inflammatory storm, tissue damage and organ failure exacerbation [6,7]. In recent years, MSCs have aroused great concern due to the biological characteristics, which confer great prospective applicability in the clinical therapy of numerous illnesses, including Systemic lupus erythematosus (SLE) [8], Type I diabetes [9], central nervous system (multiple sclerosis) [10], joints (rheumatoid arthritis) [11], liver injury [12] and lung injury [13]. Owing to the critical roles of MSCs in immunomodulation and immunosuppression, we investigated the molecular mechanisms and function of EMSC in more depth.

Studies have pointed out that intravenous infusion of MSCs in patients with ARDS can reduce lung injury by releasing various biologically active factors and interacting with damaged tissues to improve patients' long-term lung function [4]. On the other hand, Jackson [14] et al. found that MSCs block the formation of tunnel-like nanotube structures, transfer their mitochondria to macrophages to enhance the phagocytosis of macrophages, and have antibacterial and other therapeutic effects on ARDS.

On the other hand, studies have shown that the local application of MSCs can enhance endogenous cell proliferation, angiogenesis, and pyrolysis through CXCL12/CXCR4 signal axis to participate in the wound repair process [15,16]. CXCL12 is a key chemokine involved in various steady-state processes, such as neuromodulation, embryogenesis, blood vessel, and lymphocyte formation, and its expression is up-regulated during tissue healing and wound healing. Moreover, CXCL12 is the only chemokine ligand

of CXCR4, and CXCR4 is often expressed on the cell membrane of hematopoietic stem cells, lymphocytes, and bone marrow endothelial cells [17]. After CXCL12 binds to CXCR4, it promotes calcine activation and actin polymerization, thereby regulating multiple-signaling pathways, including gene transcription, cell proliferation, survival, and apoptosis, and participates in the development of immunodeficiency, inflammatory diseases, and cancer [18].

ARDS patients often show extensive alveolar epithelial injury and inflammatory edema. The latest research suggests that apoptosis and pyrolysis are critical features of ARDS alveolar injury, which may be involved in alveolar vascular endothelial injury and will lead to pulmonary blood vessels, increased permeability, low blood volume, and multiple organ failures [3,19]. Pathogen-related molecular patterns directly activate pattern recognition receptors release risk-related pattern molecules and other cytokines, resulting in the activation of transcriptional activities of NF- κ B and AP-1 and increased oxidative stress, inflammatory response, and apoptosis in cells [4,20–22]. The primary aim of this study was to identify the roles of MSCs in alveolar epithelial cells caused by ARDS and the potential mechanisms involved.

In this study, lung cell apoptosis was stimulated by TNF- α to construct an in vitro co-culture model of A549/MSCs, and an LPS-induced ARDS mouse model by tail vein injection of MSCs was built. The expression of CXCL12 and CXCR4 was knocked down to explore the effect of MSCs on ARDS cell apoptosis. We found for the first time that MSCs inhibited the apoptosis of alveolar epithelial cells caused by ARDS and exposed the mechanism exhibiting that the effects of MSCs in alveolar epithelial cells were regulated through CXCL12/CXCR4 axis.

Materials and methods

Cell culture

The human non-small cell lung cancer cell line A549 (ATCC, CCL-185) was cultured in F12K medium (Corning, 10-025-CVR) containing 10% FBS (Thermo, 10,437,085), with or without 25 ng/

mL TNF- α (Sigma, T7539), and set as TNF- α group and Vehicle group, respectively. The cells were incubated in an incubator with 5% CO₂ and 37°C for 24 hours (h). In addition, MSCs (ATCC, PCS-500-012) were cultured in DMEM low-glucose medium (Corning, 10-014-CV) containing 10% FBS in a 10% CO₂ incubator at 37°C. Cells at the logarithmic growth phase were used in subsequent experiments.

Cell co-culture

The medium for the TNF- α group and Vehicle group were first refreshed, and the Transwell chamber (Nest, 725,101) was used to establish a co-cultivation model of A549 and MSCs. MSCs were inoculated into the upper chamber of Transwell, while A549 in the TNF- α group and Vehicle group were inoculated into the lower chamber. The upper chamber contained an equal F12K medium as a control. The two chambers of cells were separated by a semi-permeable membrane but shared the same culture medium. The cells were cultured for 48 h.

Western blotting

RIPA (GBCBIO, G3424) was used to lyse cells and extract total protein to prepare protein samples. The protein lysates were separated by conventional electrophoresis, transferred onto the membrane, and washed with PBS, followed by blocking with 1% BSA for 2 h. Then, primary antibodies Box (ab32503, Abcam, Cambridge, UK), Bcl-2 (ab32124, Abcam, Cambridge, UK), Caspase-1 (ab32503, Abcam, Cambridge, UK), Cleaved Caspase-3 (ab32503, Abcam, Cambridge, UK), Caspase-8 (ab207802, Abcam, Cambridge, UK), Caspase-9 (ab2302, Abcam, Cambridge, UK), Caspase-11 (ab25901, Abcam, Cambridge, UK), Cyclin D1 (ab202068, Abcam, Cambridge, UK), ERK 1/2 (ab180673, Abcam, Cambridge, UK), p-ERK 1/2 (ab16663, Abcam, Cambridge, UK), WNT (ab17942, Abcam, Cambridge, UK), β -catenin (ab223500, Abcam, Cambridge, UK), GSDMD (ab15251, Abcam, Cambridge, UK) and β -actin (ab32572, Abcam, Cambridge, UK) (abcam, ab32503, ab32124, ab207802, ab2302, ab25901, ab202068, ab180673, ab16663, ab17942,

ab223500, ab15251, ab32572, ab219800, ab8227) each at 1:1000 dilution were incubated with the membrane overnight at 4°C. The next day, HRP (ab32572, Abcam, Cambridge, UK) and labeled IgG secondary antibody (ab150077, Abcam, Cambridge, UK) each at 1:5,000 were further incubated with the membrane at room temperature for 1 h. ECL Luminescence Kit (Thermo, 32209) was used to develop the signal in a dark room.

ELISA assay

After the cells were cultured for 24 h, the cell culture medium was taken and centrifuged at 1000 rpm for 10 min to remove the precipitate. According to the instruction of the ELISA kit (Solarbio, SEKM-0050), the expression of CXCL12 in the cell culture medium was detected. IL-1 β , TNF- α , IL-10 (Beyotime, PI301, PT512, and PI522) were employed to detect mouse serum IL-1 β , TNF- α , and IL-10 expressions. The standard wells and sample wells were set according to the instructions. After sealing the plates with the sealing film, the plates were incubated at 37°C for 30 min and then the liquid was discarded, and the plates were washed 5 times. Except for the blank wells, 50 μ l enzyme-labeled reagent was added into each well and incubated together at 37°C for 30 min. After washing, 50 μ l A and B chromogens were added for 15 min into the dark at 37°C, and finally, the reaction was terminated by adding a 50 μ l stop solution. The blank well was adjusted to 0, and the absorbance of each well was measured using a microplate reader (Biorad, iMark) within 15 min for OD value.

Lentivirus packaging

The shRNA interference fragments were designed according to the CXCR4 mRNA sequence (NM_001008540) and CXCL12 mRNA sequence (NM_000609) in GenBank. The primers were synthesized by Takara Biotechnology Co., Ltd (China), and their sequences are shown in Table 1. The pLVX-shRNA2 (Clontech, 632,179) plasmid was digested with EcoR I enzyme and BamH I, and the pLVX-CXCR4-shRNA2 plasmid was extracted by annealing and ligation. The pLVX-CXCR4-shRNA2 scramble was transfected

Table 1. Short hairpin RNA sequence of target genes.

Oligo		5'-3'
shCXCR4	Forward	5'- GGGACTATGACTCCATGAAGG-3'
	Reverse	5'- CCTTCATGGAGTCATAGTCCC-3'
shCXCL12	Forward	5'- GCATTGACCCGAAGCTAAAGT-3'
	Reverse	5'- ACTTTAGCTTCGGGTCAATGC-3'

into 293 T cells at the logarithmic growth phase using Lipo 3000 (Thermo, L3000008). MSCs were inoculated at a density of 1×10^4 per well [14], added with 2 ml F12K medium, and culture at 37°C and 5% CO₂ in saturated humidity. If the cell density reaches more than 60% the next day, the infection proceeded. After mixing 1 ml F12K medium with 1 ml corresponding virus solution, Polybrene (Sigma, TR-1003-G) was added to each well to adjust the final concentration to 2 µg/ml. After culturing for 72 h, the mixture was shaken gently and placed at 37°C in 5% CO₂ in saturated humidity. RNA was extracted from the cells, and CXCR4 expression was detected by QPCR to confirm whether the stable transgenic strain with RNA interference was constructed.

Real-time PCR

Trizol (Invitrogen, 15,596,026) was used to extract total RNA from cells, and a cDNA library was synthesized by reverse transcription with M-MLV reverse transcriptase (Thermo, AM2044). Twenty-microliter reaction system consisted of 1 µg cDNA, 0.4 µL forward and reverse primers, 10 µL $2 \times$ PerfectStartTM II Probe qPCR SuperMix (Tiangen Biochemical Technology, Beijing, FP208-01) with Nuclease-Free Water. Amplification was performed in a fluorescent quantitative PCR machine (ABI, 7500) specifically as follows: pre-denaturation 94°C for 30 sec, denaturation 94°C for 5 sec, annealing/extension at 56°C for 30 sec, for a total of 45 cycles. Three replicate wells were set up, and $2^{-\Delta\Delta C_t}$ was used to calculate the relative expressions of the target genes.

Chemotaxis assay

MSCs cells transfected with pLVX-CXCR4-shRNA2, and scramble was transferred into the upper chamber of Transwell (nest, 725,121), whereas 600 µL of F12K medium with or without

100 ng/mL CXCL12 (Thermo, PA129029) was added to the lower chamber at room temperature. After incubating for 48 hours, the colony formation in the lower chamber was observed by the colony formation experiment.

AAV-rh10 packaging

The shCXCL12 interference sequence was designed as described above [15], pAAV-rh10-ZsGreen1-shRNA, pHelper, pAAV-rh10-RC (P1619, P0243, and P0245) were purchased from Wuhan Miaoling Biotechnology Co., Ltd., AAV-rh10-ZsGreen1- CXCL12-shRNA plasmids were co-transfected with the three plasmids into AAV-rh10-293 cells (Zhongqiao Xinzhou, ZQ0334) using Lipo 3000. After 72 h of transfection, the supernatant containing AAV-rh10 particles was collected.

Conditional knockout mouse model

A total of 24 SPF-grade C57BL/6 N female Sprague-Dawley (SD) rats (Beijing Weitonglihua Experimental Animal Co., Ltd., production license SCXK (Beijing) 2016-0006) aged 6–8 weeks old and weighing 25–30 g were used. The mice were divided into four groups by random number table method as follows: Control MSCs group (MSCs group, N = 6), LPS+MSCs treatment group (LPS+MSCs group, N = 6), and shCXCR4 groups (shCXCR4+ LPS+MSCs group, N = 6) and shCXCL12 groups (shCXCL12+ LPS+MSCs group, N = 6) were transfected with the adeno-associated virus. The experiment was approved by the Animal Ethics Committee of our hospital, and all the operations were performed in compliance with the *Guiding Principles for the Protection and Use of Laboratory Animals of the National Institutes of Health* [23]. The mice were anesthetized by an intraperitoneal injection of 50 mg/kg sodium pentobarbital (Shanghai Xinya Pharmaceutical Co., Ltd., H31021725). The mouse trachea was exposed under a microscope, and the incision was then sutured after injecting the virus vector with shCXCL12 into the trachea cavity. Then the same dose of normal saline was injected into the airway of the MSCs group. The mice were

allowed to rest and recover and provided enough time develop viral infection and gene knockdown.

ARDS mouse model construction

Three weeks after establishing the conditional knockout mouse model, the mouse model of acute lung injury was established by intratracheal instillation of 50 μ L LPS (Sigma, L4130, 2 g/L). The MSCs group was given the same amount of physiological brine.

Immunofluorescence

PKH26 (Sigma, PKH26GL)-labeled MSCs transfected with shCXCR4 or scramble (5×10^6) were injected into mice with ARDS or CXCL12 knockdown three times via tail vein. The MSCs group was injected with the same amount of saline at an interval of 2 days. Fourteen days after modeling, the mice were sacrificed by cervical dislocation, and the left upper lobe tissues were quickly taken out and frozen in liquid nitrogen to prepare frozen sections. The sections were stained by DAPI (Beyotime, C1002) and mounted, and the distribution of MSCs was observed under a fluorescence microscope.

Pathological changes of lung tissues

Frozen sections of lung tissues were stained with HE and Masson, respectively. The histopathological changes were observed under a light microscope. The degree of pathological changes and mouse lung fibrosis was evaluated by The Smith score [24] and the Ashcroft score [25].

Determination of the biochemical level

According to the instructions of the kit (Beyotime, S0033S, S0131M, S0055, and S0055), the activity of reactive oxygen species ROS, lipid oxidation MDA, glutathione reductase GSH-Px, and antioxidant enzyme SOD in the cell supernatant and mouse serum were detected for evaluating the oxidative stress level of cells.

Caspase activity assay

The cells were lysed, and Caspase-1, Caspase-3, Caspase-8, and Caspase-9 kits (Beyotime, C1101, C1115, C1151, and C1157) were used to detect the activity of Caspase proteins in the cell supernatant and mouse serum. The absorbance was read at a 405 nm wavelength.

CCK-8 assay

After each group of cells was cultured for 0, 12, 24, and 48 h, cells at logarithmic growth were seeded into 96 wells at 1×10^6 [6] per well, with 6 replicate wells for each group. Ten microliters of CCK-8 (Beyotime, C0037) solution was added to each well and incubated for 2 h. A microplate reader was used to detect the absorbance of each well at 450 nm, and a cell growth curve was plotted.

CellTiter-Lumi assay

The cells were adjusted to a density of 2.5×10^4 [7] cells/ml by F12K medium and inoculated into a 96-well plate for 48 h. 100 μ L CellTiter-Lumi™ Luminescence Detection Reagent (Beyotime, C0065S) was added to each well, shaken for 2 min at room temperature and incubated for 10 min. A microplate reader was used for chemiluminescence detection.

Statistical methods

GraphPad 8 was used to draw the required pictures and perform statistical analysis. The measurement data were expressed by Mean \pm SD of three independent experiments. The independent sample t-test was performed for the comparison between groups, while the one-way analysis of variance was performed for the comparison among multiple groups. The LSD t-test was used for the post-hoc comparison. When $P < 0.05$, there is a statistical difference. All experiments were performed at least in triplicates.

Results

Although previous studies have found that MSCs have great prospective applicability in the clinical

therapy of numerous diseases, the research on the molecular mechanism of SMCs is not thoroughly investigated. Therefore, the aim of the present study was to study the effects of MSCs on the apoptosis in alveolar epithelial cells caused by ARDS and illustrate potential mechanisms underlying the effects.

TNF- α induced A549 cell apoptosis and pyrolysis and inhibited cell proliferation

The A549 cells were treated with 25 ng/ml of TNF- α for establishing an acute lung injury model in vitro. CCK-8 and Celltiter-Lumi assays showed that the proliferation and viability of the cells were decreased in time-dependent manner ($P < 0.05$) (Figure 1a-b). Compared with the Vehicle group, in the TNF- α group, the levels of ROS and MDA were increased, and the levels of SOD and GSH-px were decreased ($P < 0.05$) (Figure 1c-d), and the activities of Caspase 1, Caspase 3, Caspase 8, and Caspase 9 were significantly enhanced ($P < 0.05$) (Figure 1e). Western blot detection revealed that in the TNF- α group, the expressions of Caspase 1, Cleaved Caspase 3, Caspase 8, Caspase 9, Caspase 11, Bax, GSDMD were up-regulated, while that of Bcl-2, p-ERK1/2, WNT, β -catenin, Cyclin D1 was down-regulated (Figure 1f). These results show that TNF- α enhanced A549 cell apoptosis,

pyrolysis, and oxidation, but decreased anti-oxidation level and cell proliferation.

MSCs inhibited TNF- α -induced apoptosis and pyrolysis through the CXCL12/CXCR4 axis and promoted cell proliferation

CCK-8 and Celltiter-Lumi detected that the decreased cell proliferation and viability were reversed by the MSCs treatment ($P < 0.05$) (Figure 2a-b). Western blot results demonstrated that Caspase 9, Caspase 11, Bax, and GSDMD were down-regulated, and the expressions of Bcl-2, p-ERK1/2, WNT, β -catenin, and Cyclin D1 were up-regulated in the MSCs group (Figure 2c). After co-culture with MSCs, the levels of ROS and MDA in A549 cells treated with TNF- α were increased, the levels of SOD and GSH-px were decreased (Figure 2d-e), and the activities of Caspase 1, Caspase 3, Caspase 8, and Caspase 9 were inhibited ($P < 0.05$) (Figure 2f). ELISA showed that the expression of CXCL12 in A549 cells was up-regulated after TNF- α treatment ($P < 0.05$) (Figure 2g).

MSCs reduced pathological damage in ARDS lung tissues through CXCL12/CXCR4

Under the fluorescence microscope, we found that the number of MSCs in lung tissues of the

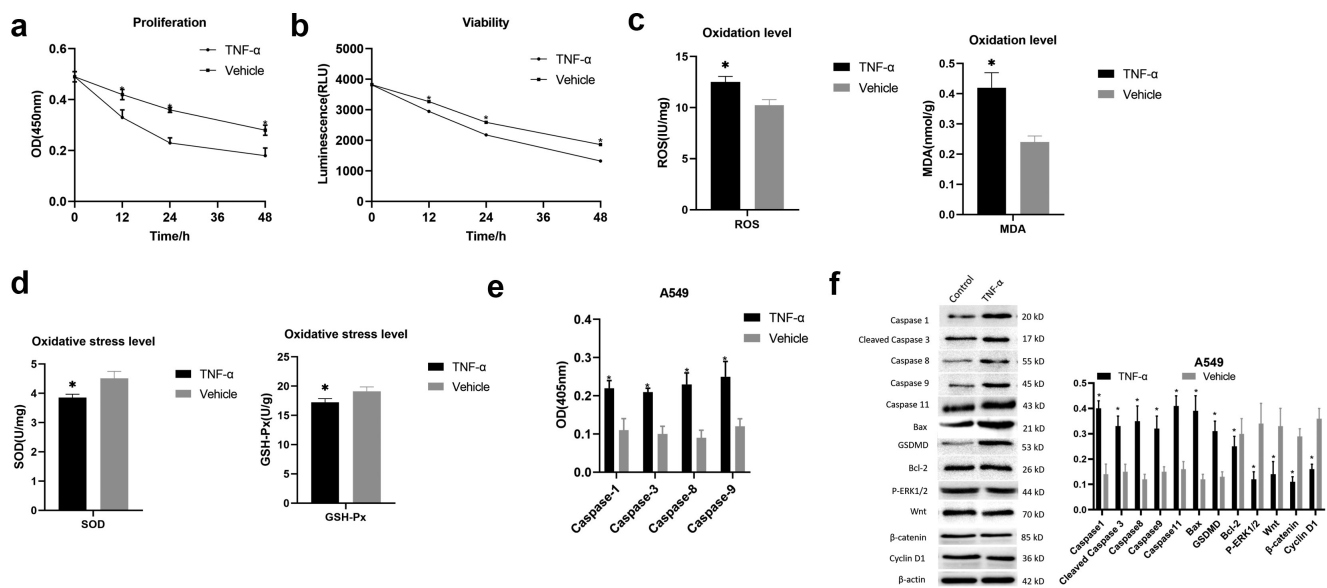


Figure 1. TNF- α induced A549 cell apoptosis. (a) CCK-8 detection of cell proliferation; (b) Celltiter-Lumi detection of cell viability; (c) Cell oxidation level detection; (d) Cell oxidation Stress level detection; (e) Caspase activity detection; (f) Western blot detection of protein expressions. Note: ** $P < 0.001$; * $P < 0.05$.

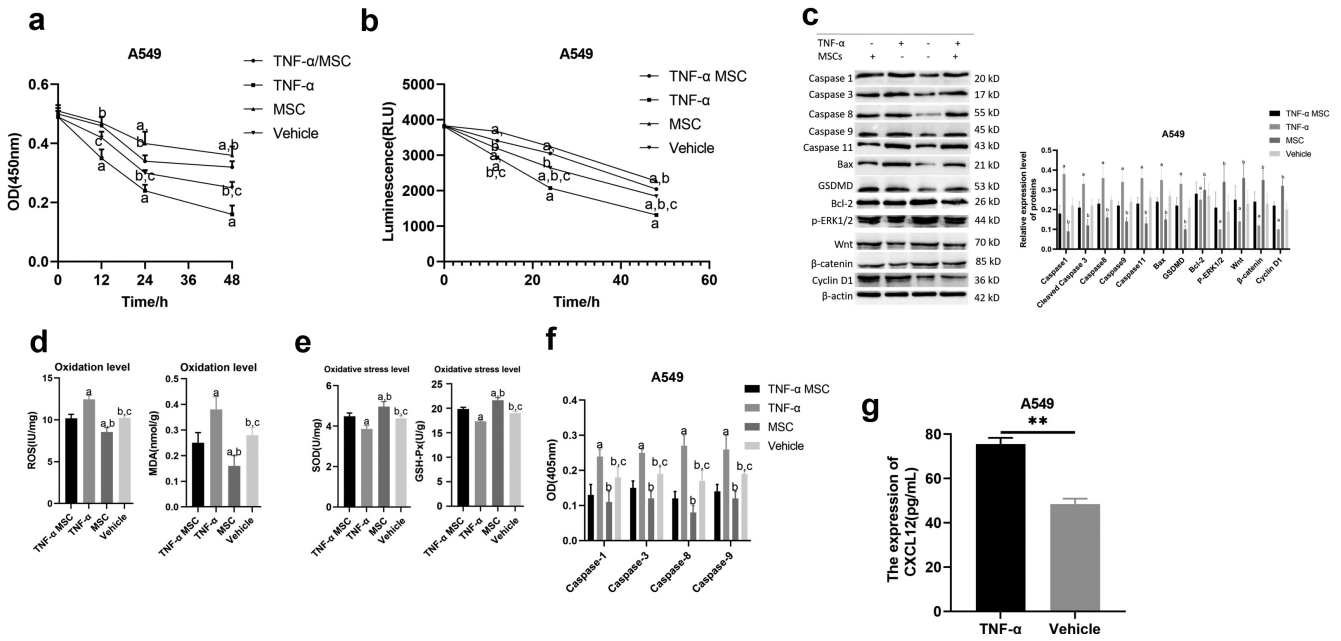


Figure 2. MSCs inhibited TNF- α -induced apoptosis. (a) CCK-8 to detect cell proliferation; (b) Celltiter-Lumi to detect cell viability; (c) Western blot detection of protein expression; (d) Cell oxidation level detection; (e) Cell oxidative stress level detection; (f) Caspase activity detection; (g) ELISA detection of CXCL12 in A549 cell culture medium. Note: [a] Compared with TNF- α /MSCs group, $P < 0.05$; [b] Compared with TNF- α group, $P < 0.05$; [c] Compared with MSCs group, $P < 0.05$; [d] Compared with Vehicle group, $P < 0.05$.

shCXCL12+ shCXCR4 group was significantly less than the shCXCL12+ MSCs group and shCXCR4 + MSCs group (Figure 3a). Moreover, mouse lung tissues of the shCXCL12+ shCXCR4 group showed extensive interstitial edema, hemorrhage and inflammatory cell infiltration, alveolar septal

fibrous tissue hyperplasia, thickening of the alveolar wall, and severe damage to the alveolar structure. And the MSCs had significantly reduced pathological damage to lung tissues and fewer collagen fibers. The lung injury score and lung fibrosis score of mice were significantly reduced

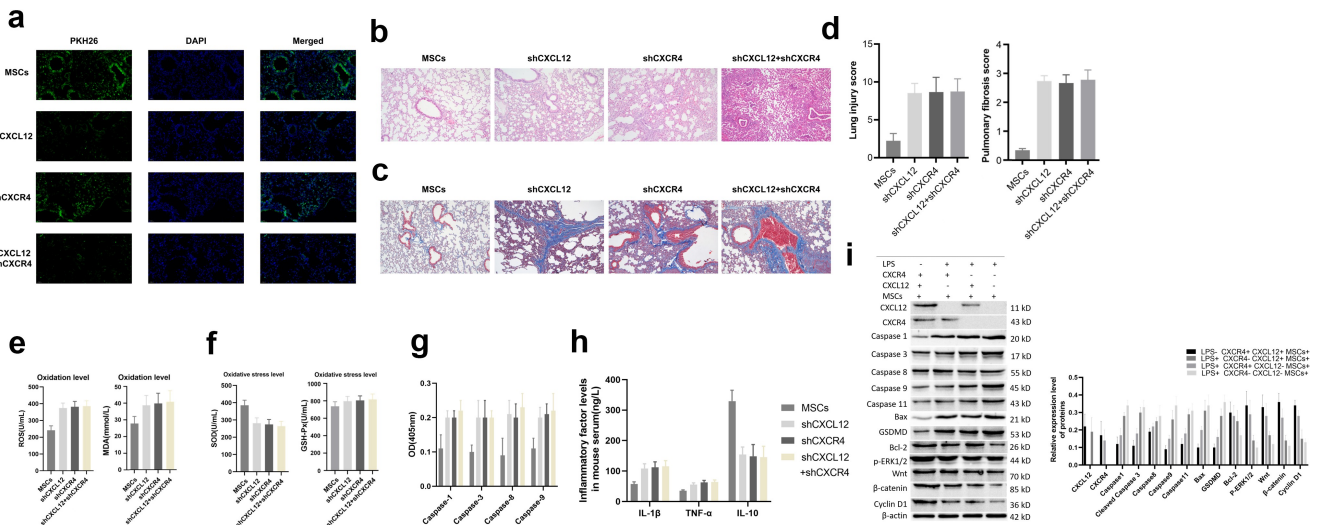


Figure 3. MSCs reduced pathological damage in ARDS lung tissues. (a) Fluorescence to observe the distribution of MSCs in mouse lung tissues; (b) HE staining to observe pathological changes and fibrosis in mouse lung tissues; (c) Masson staining to observe pathological changes and fibrosis in mouse lung tissues; (d) The lung injury score and lung fibrosis score in mouse; (e) Tissue oxidation level detection; (f) Tissue oxidative stress level detection; (g) Caspase activity detection; (h) ELISA to detect serum inflammation-related factors in mice; (i) Western blot detection of protein expressions.

($P < 0.05$), and knockdown of CXCR4 or CXCL12 can reverse the therapeutic effect of MSCs on ARDS mice (Figure 3b-d). In the shCXCL12 + shCXCR4 group, the serum levels of ROS and MDA were increased, but the levels of SOD and GSH-px were decreased ($P < 0.05$) (Figure 3e-f). The inhibition of Caspase 1, Caspase 3, Caspase 8, and Caspase 9 activities were reversed ($P < 0.05$) (Figure 3g). Compared with the MSCs group, shCXCR4 or shCXCL12 group, serum IL-1 β , and TNF- α in the shCXCL12+ shCXCR4 group were increased, and IL-10 was decreased ($P < 0.05$) (Figure 3h). And the expressions of Caspase 1, Cleaved Caspase 3, Caspase 8, Caspase 9, Caspase 11, Bax, GSDMD were up-regulated, and the expressions of Bcl-2, p-ERK1/2, WNT, β -catenin, x Cyclin D1 were down-regulated in shCXCL12 + shCXCR4 group mouse tissues (Figure 3i). After knocking out the expression of CXCR4 or (and) CXCL12, MSCs lost the repairing effect on the lung tissues of ARDS mice.

Discussion

In this study, in vivo model of an acute lung injury was established by intratracheal instillation of LPS. A549 cells were treated with TNF- α for establishing acute lung injury model in vitro. Our fluorescence results showed that MSCs were abundant in the lung tissues of ARDS mice. MSCs, which have functions of tissue repair, regeneration, and immune regulation, have shown curative effects on many diseases [26]. At present, the therapeutic effect of implanting MSCs at the injured site has been found to save damaged cells, reduce tissue damage, and accelerate cell repair by secreting many pro-survival factors. As stromal supporting cells, MSCs endogenously accelerate the self-renewal of progenitor cells, stimulate angiogenesis, and minimize apoptotic inflammatory damage [27]. However, due to the relative diameter of micro-vessels, most intravenously infused MSCs usually stay in the lung microvascular during the first circulation. This well suggests that MSCs may have a preferential therapeutic effect on lung injury. Remarkably, it has been exposed recently that MSCs play critical roles in ARDS [20]. However, the potential mechanisms underlying ARDS remain insufficient. Therefore, novel

research related to ARDS is urgently required to create new comprehension for potential therapeutic methods. Our results revealed that TNF- α stimulation might inhibit cell A549 proliferation. By contrast, MSCs treatment could reverse TNF- α -induced A549 cell proliferation, suggesting that MSCs are crucial factors in acute lung injury-induced ARDS. In vivo, MSCs had significantly reduced pathological damage to lung tissues and fewer collagen fibers.

Macrophages sense pathogen-related molecules, and risk-related pattern molecules initiate an acute host response to remove tissue debris and foreign bodies through pattern recognition receptors. However, this process often leads to mitochondrial oxidative damage, structural and metabolic damages, and activation of mitochondrial media, leading to cell apoptosis and causing excessive damage to body tissues [21,22,28]. Mitochondria are critical organelles in the process of cell death. On the one hand, under stress conditions such as the stimulation of oxidative factors such as ROS and pro-apoptotic proteins such as Bax, mitochondria lose transmembrane potential and release factors such as cytochrome C, which activates specific apoptotic signals [29]. When mitochondria are dysfunctional, the outer membrane permeability increases, releasing oxidative factors such as ROS and further causing apoptosis [30]. In addition to cell death mediated by enhanced mitochondrial permeability, Caspase-dependent cell death also attracted much research attention [29]. Caspase is a crucial protease that causes and spreads cell death signals, including apoptotic Caspase (Caspase 3, Caspase 8, Caspase 9) and inflammatory Caspase (Caspase 1, Caspase 11). After activating Caspase 8, Caspase 9, Caspase 3 will be activated to drive cell membrane vesicles, chromosomal DNA damage, and form apoptotic bodies, leading to cell apoptosis. Pyrolysis is caused by inflammatory Caspase (Caspase 1, Caspase 11). After activation, the release of IL-1 β and other inflammatory factors promotes the recruitment of monocytes to the injured site. On the other hand, GSDMD is cleaved to produce amino acid fragments. As a result, rapid cell dissolution and cytokine storms will occur. The coupling of cell lysis could cause uncontrolled pyrolysis, leading to extensive tissue damage, organ failure, and fatal

septic shock [31–33]. Several studies [34–36] have shown that in the presence of tissue damage, the ratio of Bax/Bcl-2 and release of Caspase 3, 8, 9 in the cells were increased, thereby activating cell apoptosis. However, MSCs significantly inhibited the release of cytokines. Bax, Caspase 3, 8, 9 in cells protected the cells from apoptosis induction. Another study pointed out that in an inflammatory environment, MSCs can secrete prostaglandin E2 further to promote the release of IL-10 and other anti-inflammatory factors and promote wound healing. On the other hand, it can effectively inhibit IL-1 β and GSDMD expressions to reduce pyrolysis mediated by Caspase 1 and Caspase 11 [37,38]. Our findings exposed that TNF- α stimulation might induce A549 cell apoptosis and pyrolysis, whereas MSCs could reverse TNF- α -induced A549 cell apoptosis and pyrolysis.

As reported previously, CXCL12 is up-regulated in acute lung injury, including in ARDS, and lung epithelial cells release cytokines such as CXCL12 could cause excessive neutrophils in lung tissues, stimulating tissue inflammation, damage, and fiber transformation [39,40]. The effect of administration of MSCs in vivo is directly related to the retention capacity of the corresponding tissues. Remarkably, it has been indicated recently that the homologous CXCR4 agonist CXCL12 was administered in ARDS experimental models and could produce lung protection [41]. When compared with the affinity of CXCL12, the affinity of CXCR4 was lower on lung function after isolated lung ischemia–reperfusion injury [42]. Studies have found that the overexpression of CXCR4 in MSCs can increase the chemotaxis and invasiveness of MSCs to CXCL12. Moreover, the CXCL12/CXCR4 signal axis can stimulate MSCs to aggravate injury. Some MSCs participate in the angiogenesis of the injured site and improve the efficacy of MSCs in the treatment [41,43]. Wang [44] et al. found that CXCL12 may be an anti-apoptotic factor in A549 lung cancer cells, and CXCR4 can promote CXCL12-mediated anti-apoptosis by activating JAK2/STAT3 in non-small cell lung cancer, suggesting the potential therapeutic effect of targeting CXCL12/CXCR4 signal axis on anti-apoptosis of lung cells. In this study, we found that the number of MSCs in lung tissues of the shCXCL12+ shCXCR4 group was noticeably less than the shCXCL12+ MSCs group and the shCXCR4 + MSCs group. Moreover, the shCXCL12

+ shCXCR4 group showed extensive interstitial edema, hemorrhage and inflammatory cell infiltration, alveolar septal fibrous tissue hyperplasia, thickening of the alveolar wall, and severe damage alveolar structure. Furthermore, knockdown of CXCR4 or CXCL12 could reverse the therapeutic effect of MSCs on ARDS mice, suggesting that MSCs reduced the pathological damage was through CXCL12/CXCR4 axis in ARDS. Due to the limitations of the experimental conditions, we did not discuss the specific mechanism of the MSCs-mediated CXCL12/CXCR4 signal axis, but this will be the main direction of our future research.

In addition, we also observed that MSCs significantly improved lung injury and fibrosis in ARDS mice. Under the fluorescence microscope, we found that the number of MSCs in lung tissues of the shCXCL12+ shCXCR4 group was significantly less than the shCXCL12+ MSCs group and shCXCR4 + MSCs group. MSCs can reduce the collagen differentiation and collagen deposition of fibroblasts by secreting the protein caltin-1 to maintain the stability and integrity of endothelial cells to promote tissue homeostasis [27,45]. However, Xie [42] et al. pointed out that CXCL12 can attract many CXCR4[+] fibrocytes to gather and migrate to the lung tissues to promote tissue repair and malignant fibrosis. CXCR4 is regulated by multiple cytokines and different pathways and mechanisms. Similarly, the process of MSCs-mediated CXCL12/CXCR4 may also be regulated by multiple mechanisms and factors. We hope that other scholars can explore the CXCL12/CXCR4 signal axis pairing of MSCs from different perspectives and the role of ARDS in pulmonary fibrosis. It should be noted that MSCs can promote cell proliferation and migration through the ERK and WNT/ β -catenin signaling pathways, which is often mentioned in the tissue repair effect of MSCs [46–48], suggesting that MSCs can affect ARDS tissues. Moreover, the tissue repair effect of MSCs is likely to be achieved by promoting cell proliferation.

Conclusions

In conclusion, our results demonstrate that TNF- α enhanced A549 cell apoptosis, pyrolysis, and oxidation, but decreased anti-oxidation level and cell proliferation. In addition, MSCs could inhibit TNF- α -induced apoptosis and pyrolysis, promote cell

proliferation, and reduce pathological damage in ARDS lung tissues through CXCL12/CXCR4 signal axis. In summary, MSCs could inhibit TNF- α and LPS-induced lung cell apoptosis through the CXCL12/CXCR4 signal axis to improve lung tissue damage and pulmonary fibrosis in ARDS mice. These findings afford novel insight into intervention targets for MSCs in ARDS.

Disclosure statement

No potential conflict of interest was reported by the author(s).

Funding

General Project of Hunan Natural Science Foundation (No.2019JJ40287) and Xiangtan Medical Research Project (No.2020xtyx-15).

References

- [1] Fan E, Brodie D, Slutsky A. Acute respiratory distress syndrome: advances in diagnosis and treatment. *Jama*. 2018;319(7):698–710.
- [2] Rezoagli E, Fumagalli R, Bellani G. Definition and epidemiology of acute respiratory distress syndrome. *Ann Transl Med*. 2017;5(14):282.
- [3] Matthay MA, Zemans RL, Zimmerman GA, et al. Acute respiratory distress syndrome. *Nat Rev Dis Primers*. 2019;5(1):1–22.
- [4] Thompson BT, Chambers RC, Liu KD. Acute respiratory distress syndrome. *N Engl J Med*. 2017;377(6):562–572.
- [5] Beitler JR, Thompson BT, Baron RM, et al. Advancing precision medicine for acute respiratory distress syndrome. *Lancet Respir Med*. 2022;10(1):107–120.
- [6] Najj A, Favier B, Deschaseaux F, et al. Mesenchymal stem/stromal cell function in modulating cell death. *Stem Cell Res Ther*. 2019;10(1):56.
- [7] Moll G, Hoogduijn MJ, Ankrum JA. Safety, efficacy and mechanisms of action of mesenchymal stem cell therapies. *Front Immunol*. 2020;11:11.
- [8] Woodworth TG, Furst DE. Safety and feasibility of umbilical cord mesenchymal stem cells in treatment-refractory systemic lupus erythematosus nephritis: time for a double-blind placebo-controlled trial to determine efficacy. *Arthritis Res Ther*. 2014;16(4):113.
- [9] Bhone RR, Sheshadri P, Sharma S, et al. Making surrogate β -cells from mesenchymal stromal cells: perspectives and future endeavors. *Int J Biochem Cell Biol*. 2014;46:90–102.
- [10] Ghannam S, Bouffi C, Djouad F, et al. Immunosuppression by mesenchymal stem cells: mechanisms and clinical applications. *Stem Cell Res Ther*. 2010;1(1):2.
- [11] Dorronsoro A, Fernández-Rueda J, Fechter K, et al. Human mesenchymal stromal cell-mediated immunoregulation: mechanisms of action and clinical applications. *Bone Marrow Res*. 2013;2013:203643.
- [12] Xu L, Gong Y, Wang B, et al. Randomized trial of autologous bone marrow mesenchymal stem cells transplantation for hepatitis B virus cirrhosis: regulation of Treg/Th17 cells. *J Gastroenterol Hepatol*. 2014;29(8):1620–1628.
- [13] Simonson OE, Mouggiakakos D, Heldring N, et al. In vivo effects of mesenchymal stromal cells in two patients with severe acute respiratory distress syndrome. *Stem Cells Transl Med*. 2015;4(10):1199–1213.
- [14] Jackson MV, Morrison TJ, Doherty DF, et al. Mitochondrial transfer via tunneling nanotubes is an important mechanism by which mesenchymal stem cells enhance macrophage phagocytosis in the in vitro and in vivo models of ARDS. *Stem Cells*. 2016;34(8):2210–2223.
- [15] Wang X, Jiang B, Sun H, et al. Noninvasive application of mesenchymal stem cell spheres derived from hESC accelerates wound healing in a CXCL12-CXCR4 axis-dependent manner. *Theranostics*. 2019;9(21):6112.
- [16] Ding J, Cui X, Liu Q. Emerging role of HMGB1 in lung diseases: friend or foe. *J Cell Mol Med*. 2017;21(6):1046–1057.
- [17] Janssens R, Struyf S, Proost P. The unique structural and functional features of CXCL12. *Cell Mol Immunol*. 2018;15(4):299–311.
- [18] García-Cuesta EM, Santiago CA, Vallejo J, et al. The role of the CXCL12/CXCR4/ACKR3 axis in autoimmune diseases. *Front Endocrinol (Lausanne)*. 2019;10:585.
- [19] Cheng KT, Xiong S, Ye Z, et al. Caspase-11-mediated endothelial pyroptosis underlies endotoxemia-induced lung injury. *J Clin Invest*. 2017;127(11):4124–4135.
- [20] Pooladanda V, Thatikonda S, Bale S, et al. Nimbolide protects against endotoxin-induced acute respiratory distress syndrome by inhibiting TNF- α mediated NF- κ B and HDAC-3 nuclear translocation. *Cell Death Dis*. 2019;10(2):1–17.
- [21] Ooppachai C, Limtrakul Dejkriengkraikul P, Yodkeeree S. Dicentrine potentiates TNF- α -induced apoptosis and suppresses invasion of A549 lung adenocarcinoma cells via modulation of NF- κ B and AP-1 activation. *Molecules*. 2019;24(22):4100.
- [22] Patel MN, Carroll RG, Galván-Peña S, et al. Inflammasome priming in sterile inflammatory disease. *Trends Mol Med*. 2017;23(2):165–180.
- [23] Toussaint I. Alternative methods for killing laboratory animals: summary of a published advisory report by the Netherlands national Committee for the protection of animals used for scientific purposes and for education (NCad). *Lab Anim*. 2017;51(2):222–223.
- [24] Ding Q, Liu G, Zeng Y, et al. Glycogen synthase kinase-3 β inhibitor reduces LPS-induced acute lung injury in mice. *Mol Med Rep*. 2017;16(5):6715–6721.

- [25] Islam D, Huang Y, Fanelli V, et al. Identification and modulation of microenvironment is crucial for effective mesenchymal stromal cell therapy in acute lung injury. *Am J Respir Crit Care Med.* 2019;199(10):1214–1224.
- [26] Su W, Wan Q, Huang J, et al. Culture medium from TNF- α -stimulated mesenchymal stem cells attenuates allergic conjunctivitis through multiple antiallergic mechanisms. *J Allergy Clin Immunol.* 2015;136(2):423–432. e8.
- [27] S J L, Lee RH, Gregory CA. Mechanisms of mesenchymal stem/stromal cell function. *Stem Cell Res Ther.* 2016;7(1):125.
- [28] Zhong Z, Umemura A, Sanchez-Lopez E, et al. NF- κ B restricts inflammasome activation via elimination of damaged mitochondria. *Cell.* 2016;164(5):896–910.
- [29] Liu D, Perfettini JL, Brenner C. Mitochondrial regulation of cell death mitochondrial biology and experimental therapeutics. Cham: Springer; 2018. p. 75–90.
- [30] Hong Duck M. Bcl-2 family proteins as regulators of cancer cell invasion and metastasis: a review focusing on mitochondrial respiration and reactive oxygen species. *Oncotarget.* 2016;7(5):5193.
- [31] Ramierz MLG, Salvesen GS. A primer on caspase mechanisms Seminars in cell & developmental biology. Vol. 82. La Jolla, CA: Academic Press; 2018. p. 79–85.
- [32] Fritsch M, Günther SD, Schwarzer R, et al. Caspase-8 is the molecular switch for apoptosis, necroptosis and pyroptosis. *Nature.* 2019;575(7784):683–687.
- [33] Huang X, Feng Y, Xiong G, et al. Caspase-11, a specific sensor for intracellular lipopolysaccharide recognition, mediates the non-canonical inflammatory pathway of pyroptosis. *Cell Biosci.* 2019;9(1):31.
- [34] Li S, Qi Y, Hu S, et al. Mesenchymal stem cells-conditioned medium protects PC12 cells against 2, 5-hexanedione-induced apoptosis via inhibiting mitochondria-dependent caspase 3 pathway. *Toxicol Ind Health.* 2017;33(2):107–118.
- [35] Li CL, Leng Y, Zhao B, et al. Human iPSC-MSC-derived xenografts modulate immune responses by inhibiting the cleavage of caspases. *Stem Cells.* 2017;35(7):1719–1732.
- [36] Li L, Wang R, Jia Y, et al. Exosomes derived from mesenchymal stem cells ameliorate renal ischemic-reperfusion injury through inhibiting inflammation and cell apoptosis. *Front Med (Lausanne).* 2019;6:6.
- [37] Schneider KS, Groß C J, Dreier RF, et al. The inflammasome drives GSDMD-independent secondary pyroptosis and IL-1 release in the absence of caspase-1 protease activity. *Cell Rep.* 2017;21(13):3846–3859.
- [38] Liu Y, Li P, Qiao C, et al. Chitosan hydrogel enhances the therapeutic efficacy of bone marrow-derived mesenchymal stem cells for myocardial infarction by alleviating vascular endothelial cell pyroptosis. *J Cardiovasc Pharmacol.* 2020;75(1):75–83.
- [39] Isles HM, Herman KD, Robertson AL, et al. The CXCL12/CXCR4 signaling Axis retains neutrophils at inflammatory sites in zebrafish. *Front Immunol.* 2019;10:1784.
- [40] Hammad H, Lambrecht BN. Rbm7 in structural cells: a NEAT way to control fibrosis. *Immunity.* 2020;52(3):429–431.
- [41] Li Z, Wang W, Xu H, et al. Effects of altered CXCL12/CXCR4 axis on BMP2/Smad/Runx2/Osterix axis and osteogenic gene expressions during osteogenic differentiation of MSCs. *Am J Transl Res.* 2017;9(4):1680.
- [42] Xie L, Zhao L. Role of CXCL12/CXCR4-Mediated Circulating Fibrocytes in Pulmonary Fibrosis. *Journal of Biomedicine.* 2017;2:134–139.
- [43] Zheng XB, He XW, Zhang LJ, et al. Bone marrow-derived CXCR4-overexpressing MSCs display increased homing to intestine and ameliorate colitis-associated tumorigenesis in mice. *Gastroenterol Rep (Oxf).* 2019;7(2):127–138.
- [44] Wang M, Lin T, Wang Y, et al. CXCL12 suppresses cisplatin-induced apoptosis through activation of JAK2/STAT3 signaling in human non-small-cell lung cancer cells. *Onco Targets Ther.* 2017;10:3215.
- [45] El Agha E, Kramann R, Schneider RK, et al. Mesenchymal stem cells in fibrotic disease. *Cell Stem Cell.* 2017;21(2):166–177.
- [46] Ma T, Fu B, Yang X, et al. Adipose mesenchymal stem cell-derived exosomes promote cell proliferation, migration, and inhibit cell apoptosis via Wnt/ β -catenin signaling in cutaneous wound healing. *J Cell Biochem.* 2019;120(6):10847–10854.
- [47] Zhou X, Li T, Chen Y, et al. Mesenchymal stem cell-derived extracellular vesicles promote the in vitro proliferation and migration of breast cancer cells through the activation of the ERK pathway. *Int J Oncol.* 2019;54(5):1843–1852.
- [48] Ren S, Chen J, Duscher D, et al. Microvesicles from human adipose stem cells promote wound healing by optimizing cellular functions via AKT and ERK signaling pathways. *Stem Cell Res Ther.* 2019;10(1):47.